

Random Wave-Induced Pore Pressure Accumulation in Marine Soils

Y.-T. Tsai

Assistant Professor.

W. G. McDougal

Associate Professor.

Department of Civil Engineering,
Oregon State University
Corvallis, OR 97331

Random wave-induced pore pressure is examined using linear superposition, Miner's method and a single representative wave. Solutions are developed for deep and shallow soils. A deep soil has a higher liquefaction potential than a shallow soil for the same wave conditions. Linear superposition, Miner's method and using the rms wave height are in general agreement for the deep soil. The significant wave overestimates the liquefaction potential and should not be used. There was poor agreement among the methods for a shallow soil.

1 Introduction

Wave-induced cyclic shear stresses in the seabed may cause a pore pressure accumulation which reduces the strength of the soil. If the pore pressure continues to accumulate, there will be a total loss of strength and the soil liquefies. This response is well documented in earthquake engineering for loosely packed, fine-grained, saturated, cohesionless soils (Seed and Idriss, 1967). A typical marine failure is the flotation of a 10-ft-dia steel pipe in Lake Ontario which occurred when the backfill liquefied during storms (Christian et al., 1974).

The wave-induced pore pressure accumulation in marine soils has been the subject of several studies. This paper discusses the techniques used to examine pressure accumulation due to random waves. Common techniques include time domain solutions, Miner's rule, superposition and selection of a single representative wave. To facilitate a direct comparison of these, a modified version of the pressure accumulation model proposed by Seed and Rahman (1978) is employed. They developed a finite element model for an infinitely deep soil to estimate the time history of pore pressure response to a selected design storm. The model is based on the one-dimensional storage equation, assuming that the volume change is caused by the change of effective bulk stress, which is produced by the dissipation of pore pressure from the soil element. This yields the one-dimensional Terzaghi consolidation equation with a pore pressure generation source term.

McDougal and Liu (1986) gave an analytical solution for the consolidation equation. Two models for the pressure source term were also developed corresponding to deep and shallow soils. McDougal et al. (1989) compared these models with wave tank experiments and found reasonable agreement for cases when the soil liquefied.

Rahman and Layas (1986) have also presented an analytic solution to the consolidation equation. A stochastic model was developed to evaluate the expected damage associated

with the progressive accumulation of pore pressure. It was observed that the maximum expected damage occurred at some depth below the ocean floor. However, there appears to be a discrepancy between the presented equations and figures for the pore pressure ratio at the mudline.

In this paper, analytical solutions are used in conjunction with the source terms developed by McDougal and Liu (1986) to evaluate the random wave-induced pore pressure accumulation. Since the solution is linear, three methods of examining random forcing are considered: superposition, Miner's method, and a single representative wave.

2 Theory

Only an overview of the analytical solution to the earthquake consolidation is given. More details may be found in McDougal and Liu (1986) and Rahman and Layas (1986). The initial-boundary value problem is given as

$$\frac{\partial u}{\partial t} = c \frac{\partial^2 u}{\partial z^2} + \psi \quad (1a)$$

$$u(0, t) = 0 \quad (1b)$$

$$\frac{\partial}{\partial z} u(d, t) = 0 \quad (1c)$$

$$u(z, 0) = 0 \quad (1d)$$

where u is the mean pore pressure, t is time, c is the coefficient of consolidation, z is the vertical coordinate axis as shown in Fig. 1, and ψ is the source term representing the function which gives the rate of pore pressure generation resulting from the action of cyclic shear stress under undrained conditions. The mudline boundary condition is that the wave-induced dynamic pressure time averages to zero. The bottom boundary condition assumes that the soil layer of thickness d is overlying a rigid impermeable bed, as shown in Fig. 1. The initial condition is no excess pressure.

To develop simple analytical solutions, the deep and shallow water limits of linear wave theory are examined. The

Contributed by the OMAE Division for publication in the JOURNAL OF OFFSHORE MECHANICS AND ARCTIC ENGINEERING. Manuscript received by the OMAE Division, November 18, 1988; revised manuscript received October 25, 1989.

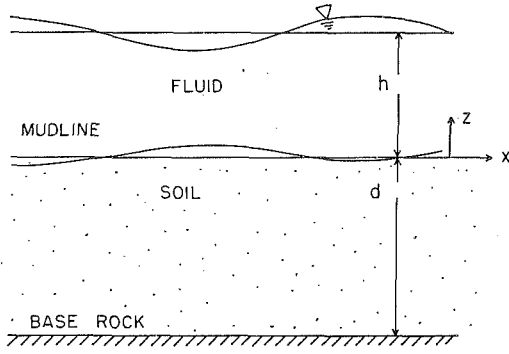


Fig. 1 Definition sketch

source terms for a deep soil ($d/L > 1/2$) and a shallow soil ($d/L < 1/20$), where L is the wavelength, were given by McDougal et al. (1989) as

$$\psi^D = \frac{\gamma_B}{\tau} \left(\frac{1 + 2k_o}{3} \right)^{1+1/\beta} \left(\frac{1}{\alpha} \frac{P_o \lambda}{\gamma_B} \right)^{-1/\beta} z e^{\lambda z / \beta} \quad (2a)$$

$$\psi^S = \frac{\gamma_B}{\tau} \left(\frac{1 + 2k_o}{3} \right)^{1+1/\beta} \left(\frac{1}{\alpha} \frac{m}{\gamma_B} \right)^{-1/\beta} z e^{\lambda z / \beta} \quad (2b)$$

where γ_B is the buoyant weight density of the soil, and k_o is the coefficient of lateral earth pressure, τ is the wave period, P_o is the mudline pressure amplitude; λ is the wave number, m is the slope of the cyclic shear stress profile, and α and β are empirical coefficients determined from the cyclic strength curve. Solutions to (1) are given by

$$u = \sum_{n=0}^{\infty} F_n (1 - e^{-ck_n^2 t}) \sin k_n z \quad (3a)$$

where, for the deep soil,

$$F_n = \frac{2}{d} \frac{\gamma_B}{\tau c k_n^2} \left(\frac{1 + 2k_o}{3} \right)^{1+1/\beta} \left(\frac{P_o \lambda}{\alpha \gamma_B} \right)^{-1/\beta} \quad (3b)$$

$$\left\{ \frac{\sin(k_n d) e^{\lambda d / \beta}}{\left(\frac{\lambda}{\beta} \right)^2 + k_n^2} \left[\frac{k d}{\beta} + \frac{k_n^2 - \left(\frac{\lambda}{\beta} \right)^2}{\left(\frac{\lambda}{\beta} \right)^2 + k_n^2} \right] - \frac{2 k_n \lambda / \beta}{\left[\left(\frac{\lambda}{\beta} \right)^2 + k_n^2 \right]^2} \right\}$$

and for the shallow soil

$$F_n = \frac{2}{d} \frac{\gamma_B}{\tau c k_n^2} \left(\frac{1 + 2k_o}{3} \right)^{1+1/\beta} \left(\frac{1}{\alpha} \frac{m}{\gamma_B} \right)^{-1/\beta} \frac{\sin(k_n d)}{k_n^2} \quad (3c)$$

with

$$k_n = \frac{(2n + 1)\pi}{2d} \quad (3d)$$

The ratio of the pore pressure accumulation to the effective overburden is an indicator of liquefaction potential. The pore pressure ratio is given by

$$r = \frac{u}{\sigma_o} \quad (4a)$$

where the effective overburden is

$$\sigma_o = \gamma_B z \left(\frac{1 + 2k_o}{3} \right) \quad (4b)$$

When r exceeds 0.13 to 0.20, the soil is assumed to fail due to liquefaction.

3 Random Wave-Induced Pressure Accumulation

Three methods which can be used to predict the random wave-induced liquefaction are superposition, Miner's method, and selecting a single representative wave. Profiles of a random sea at a fixed point can be expressed as the linear superposition of an infinite number of regular wave components.

$$\eta(t) = \sum_{i=1}^{\infty} a_i \cos(2\pi f_i t + \epsilon_i) \quad (5)$$

in which η is the wave profile and a_i , f_i , and ϵ_i are the wave amplitude, frequency, and phase angle of the i th component wave. The component amplitudes are related to the wave energy spectrum density $S(f_i)$ by

$$\frac{a_i^2}{2\Delta f_i} = S(f_i) \quad (6)$$

where Δf_i is the frequency interval. The components of wave amplitude can be obtained from (6).

In this study, these methods are compared using a Bretschneider spectrum. This two-parameter spectrum is given as

$$S(f) = \frac{5H_s^2}{16f_o} \frac{1}{(f/f_o)^5} \exp \left[-\frac{5}{4} \left(\frac{f}{f_o} \right)^4 \right] \quad (7a)$$

in which H_s is the significant wave height; f is the frequency; and f_o is the peak frequency, which is related to the significant wave period by

$$f_o = 0.946/T_s \quad (7b)$$

3.1 Superposition. The superposition technique has been employed to examine a variety of problems such as wave forces, refraction, and diffraction. This technique is also employed in this paper to estimate the liquefaction potential induced by random waves.

The total wave energy density of a random sea is given by

$$E = \gamma_w \int_0^{\infty} S(f) df \approx \frac{\gamma_w}{8} \sum_{i=1}^{\infty} H_i^2 \quad (8)$$

where H_i is the i th component wave height, and γ_w is the weight density of water. The total energy is independent of the number of wave components, if the number is sufficiently large.

The pore pressure ratio for a deep soil layer using (3) and (4) is

$$r^D = \frac{2}{d} \frac{1}{\tau z} \left(\frac{1 + 2k_o}{3} \right)^{1/\beta} \left(\frac{\lambda}{\alpha \gamma_B} \right)^{-1/\beta} \cdot R_n^D \left[\frac{\gamma_w H}{2ch(\lambda h)} \right]^{-1/\beta} \quad (9a)$$

in which the mudline wave pressure is given as

$$P_o = \frac{\gamma_w H}{2ch(\lambda h)} \quad (9b)$$

and

$$R_n^D = \sum_{n=0}^{\infty} \frac{1}{c k_n^2} \left\{ \frac{\sin(k_n d) e^{\lambda d / \beta}}{\left(\frac{\lambda}{\beta} \right)^2 + k_n^2} \left[\frac{\lambda d}{\beta} + \frac{k_n^2 - \left(\frac{\lambda}{\beta} \right)^2}{\left(\frac{\lambda}{\beta} \right)^2 + k_n^2} \right] - \frac{2 k_n \lambda / \beta}{\left[\left(\frac{\lambda}{\beta} \right)^2 + k_n^2 \right]^2} \right\} (1 - e^{-ck_n^2 t}) \sin(k_n z) \quad (9c)$$

where h is the water depth.

The exponent of wave height in (9a) is taken as 1, so that the pore pressure ratio is related to the energy of each wave component.

$$(r^D)^{-\beta} = [g^D(f)]a \quad (10a)$$

where

$$[g^D(f)]^2 = \left(\frac{2}{d} \frac{R_n^D}{\tau z}\right)^{-2\beta} \left(\frac{1+2k_o}{3}\right)^{-2} \left[\frac{\gamma_w \lambda}{\alpha \gamma_B c h(\lambda h)}\right]^2 \quad (10b)$$

Considering the component waves and substituting (10a) into (8) yields

$$E = \frac{\gamma_w}{8} \sum_{i=1}^{\infty} \frac{(r_i^D)^{-2\beta}}{g(f_i)} \quad (11)$$

Defining the total wave-induced pore pressure ratio as r^D , it follows by analogy with the total wave energy that

$$\frac{\gamma_w}{8} \frac{(r^D)^{-2\beta}}{g(f)} = \frac{\gamma_w}{8} \sum_{i=1}^{\infty} \frac{(r_i^D)^{-2\beta}}{g(f_i)} \quad (12)$$

If it is assumed that

$$g^D(f) \propto g^D(f_o) \quad (13)$$

then

$$(r^D)^{-2\beta} = g^D(f_o) \sum_{i=1}^{\infty} H_i^2 \quad (14)$$

The equation states that the pore pressure ratio is proportional to the total energy in the spectrum.

Consequently, the random wave-induced pore pressure accumulation ratio is given by

$$r^D = \left[g^D(f_o) \sum_{i=1}^{\infty} H_i^2 \right]^{-(1/2,\beta)} \quad (15)$$

Following similar steps for the deep soil model, the shallow soil pore pressure ratio can also be developed for random waves. The result is

$$r^S = \left[g^S(f_o) \sum_{i=1}^{\infty} H_i^2 \right]^{-(1/2,\beta)} \quad (16a)$$

where

$$g^S(f_o) = \left(\frac{2}{d} \frac{R_n^S}{\tau z}\right)^{-2\beta} \left(\frac{1+2k_o}{3}\right)^{-2} \left[\frac{\gamma_w m_c}{2\alpha \gamma_B c h(\lambda h)}\right]^2 \quad (16b)$$

in which

$$R_n^S = \sum_{n=0}^{\infty} \frac{1}{ck_n^2} \frac{\sin(k_n d)}{k_n^2} (1 - e^{-ck_n^2 t}) \sin(k_n z) \quad (16c)$$

and m_c is a function of the wave and soil conditions and is given in McDougal and Liu (1986).

Numerical results for a soil with the properties listed in Table 1 are presented. The wave conditions are taken as $H_s = 5.0$ m, $T_s = 10.0$ s, and $h = 10.0$ m. The spectrum is shown in Fig. 2. The soil depths are 50 m for the deep soil and 4 m for the shallow soil.

Figures 3(a) and 3(b) show the pore pressure ratio profiles at different times for deep and shallow soil, respectively. For deep soil, there is a high potential for liquefaction near the mudline. The potential monotonically decreases with the depth. The liquefaction potential is very low in the shallow

soil and no failure is expected. Figures 4(a) and 4(b) present the data to more clearly demonstrate the time history of the liquefaction potential. The pore pressure accumulation in the deep soil takes a longer time to reach a steady state than the shallow soil. This time difference is because the deep soil has a greater capacity to accumulate pressure.

Table 1 Assumed soil properties (medium dense sand)

Dimensionless coefficients	$\alpha = 0.246$
	$\beta = -0.165$
Relative density	$D_r = 54$ percent
Coefficient of consolidation	$c = 0.03$ m ² /s
Poisson's ratio	$\nu = 0.3$
Buoyant weight density of soil	$\gamma_B = 8.5$ KN/m ³
Coefficient of lateral earth pressure	$k_o = 0.5$

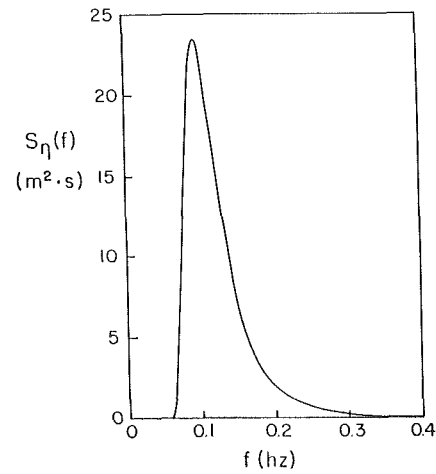
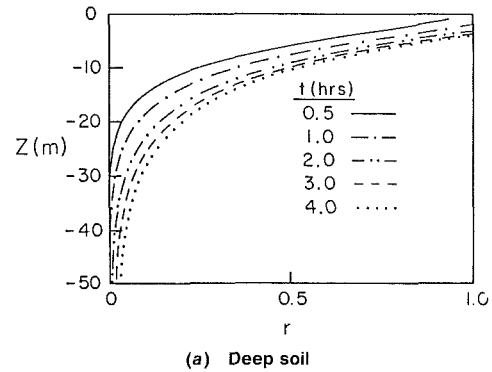
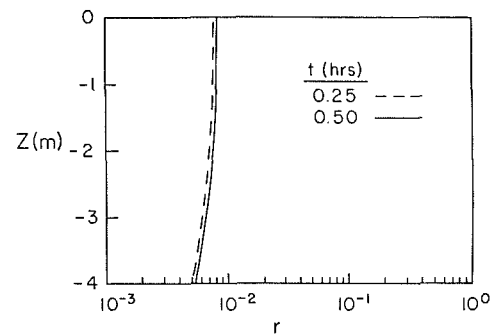


Fig. 2 Bretschneider spectrum for $H_s = 5.0$ m and $T_s = 10.0$ s



(a) Deep soil



(b) Shallow soil

Fig. 3 Pore pressure ratio profiles form superposition method

Figure 5 shows the shear stress versus the relative soil depth with the layer depth as a parameter. Obviously, the shear stress in the shallow soil is much smaller than that in the deep soil, especially near the mudline. This low stress in the shallow soil is why there is a lower liquefaction potential in the shallow soil.

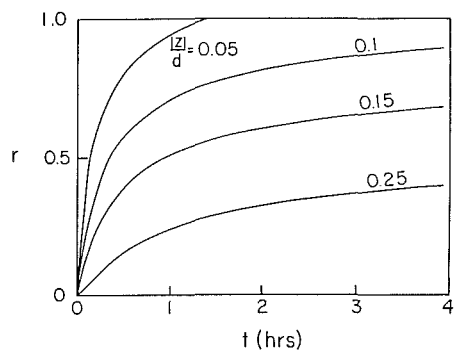
3.2 Miner's Method. Earthquake engineers have used Miner's method (Lee and Chan, 1972) to predict earthquake-induced liquefaction. This method converts the random shear stress to an equivalent number of uniform stresses with an average shear stress which is defined by 65 percent of the maximum stress. In this method, time history of shear stress at different layers of the soil and the cyclic strength curve are required.

Figure 6 is the time history of a 10-min wave-train-induced shear stress at a depth of 5 m in the deep soil. To employ

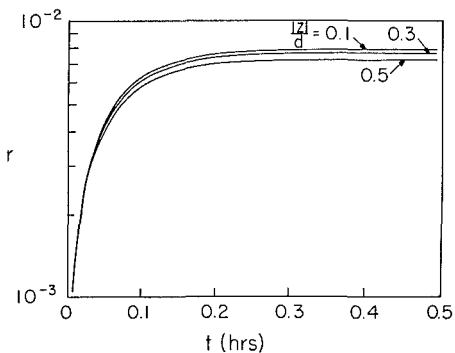
Miner's method the stress histories at a number of depths were analyzed. The shear stress is induced by the random wave pressure along the mudline which is generated by using the Bretschneider spectrum. The results for a deep soil are shown in Fig. 7(a). There is liquefaction potential in approximately the upper 15 percent of the soil depth.

The shallow soil case is also analyzed. The result is shown in Fig. 7(b). Although there is no liquefaction, the actual shear stress is very close to the shear stress causing liquefaction. This is not predicted by the superposition method.

3.3 Single Representative Wave. The significant wave has been widely used as a design wave in coastal and ocean engineering. It is the wave corresponding to the average of the highest one-third of the waves in the spectrum. The height and period are considered to be representatives of a random wave train. The significant wave may contain as much as twice the energy as the spectrum. Thus a large pore pressure accumulation is anticipated for the significant wave. The root mean square wave height properly represents the total energy in the spectrum. Pore pressure ratio profiles using these two



(a) Deep soil



(b) Shallow soil

Fig. 4 Time history of pore pressure development by superposition method

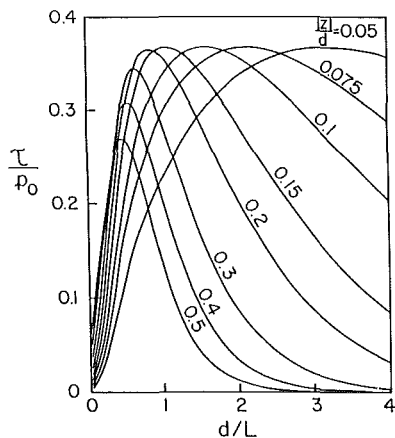


Fig. 5 Cyclic shear stress as a function of the relative soil depth

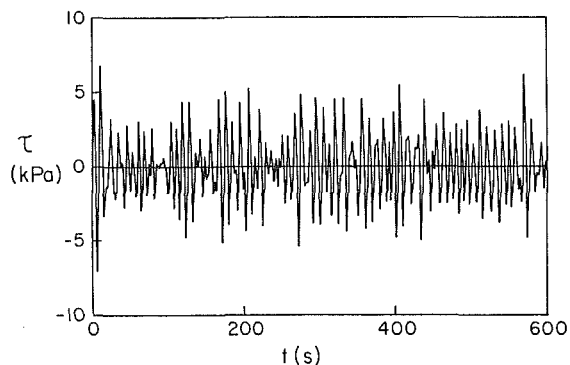
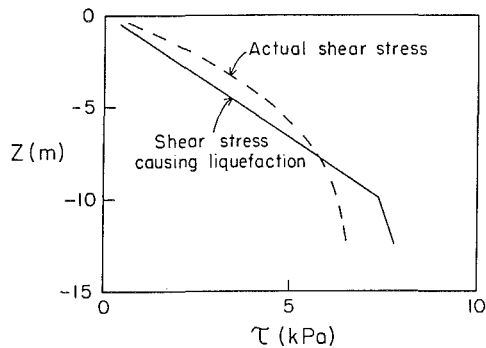
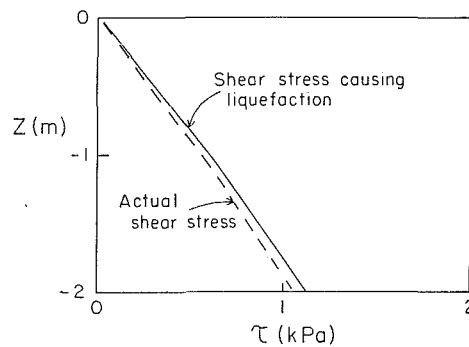


Fig. 6 Time history of cyclic shear stress at a depth of 5 m in a deep soil



(a) Deep soil



(b) Shallow soil

Fig. 7 Liquefaction estimates using Miner's method

waves are shown in Figs. 8 and 9 for the deep and shallow soil cases. If the peak frequency is chosen as the frequency for the rms wave, then the pore pressure accumulation prediction by using the rms wave method is identical to the prediction by the superposition method.

4 Conclusions

Random wave-induced pore pressure accumulation in the ocean bed is evaluated by three methods: superposition, Miner's method, and single representative wave. The depth and time-dependent development of the liquefaction potential for a Bretschneider spectrum was examined for deep and shallow soils. It is found that the deep soil had a higher liquefaction potential than the shallow soil under the same wave conditions; this is because the wave-induced shear stress is lower in the shallow soil. The superposition method, Miner's method, and the rms wave are all in reasonable agreement for the deep soil case. The significant wave overestimates liquefaction potential and should not be used to estimate the liquefaction potential. There was poor agreement among the methods for the shallow soil case.

Acknowledgments

This research was initially supported by the Oregon State University Sea Grant College Program, National Oceanic and

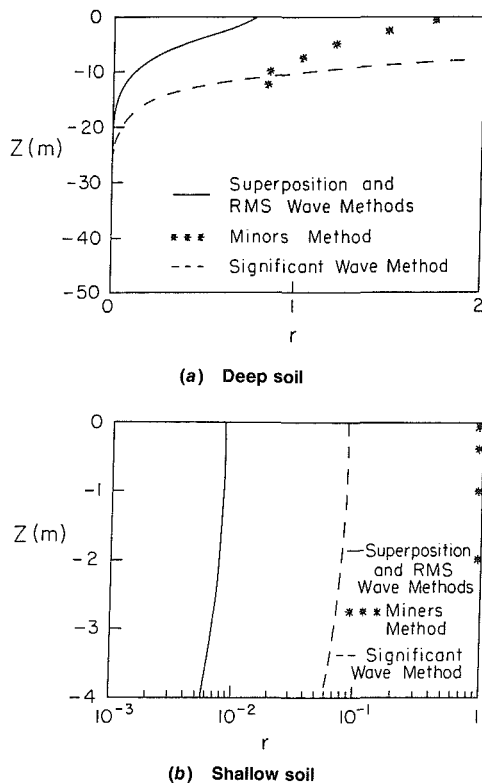


Fig. 8 Comparison of liquefaction estimates for three methods (storm duration = 10 min)

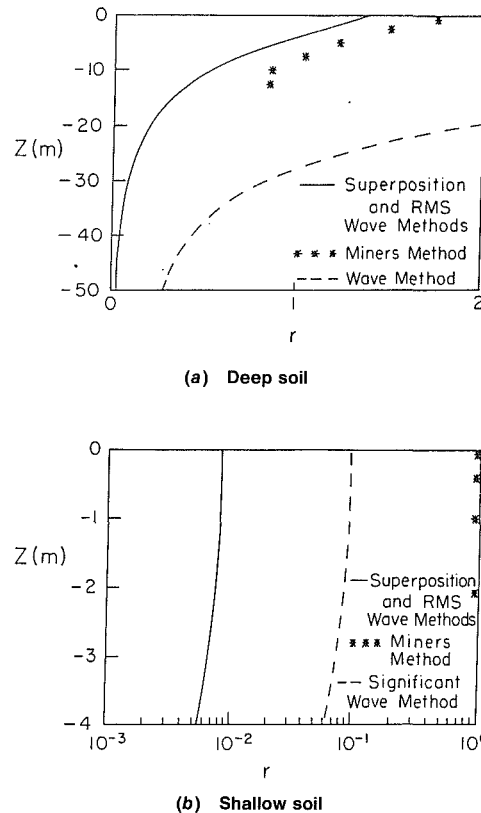


Fig. 9 Comparison of liquefaction estimates for three methods (storm duration = 4 hr)

Atmospheric Administration Office of Sea Grant, Department of Commerce under Grant No. NA81AA-D-00-086 (Project No. R/CE-13). Later support was provided by the Office of Naval Research under the University Research Initiative (URI) Contract No. N00014-86-0687.

References

- Christian, J. T., Taylor, P. K., Yen, J. K. C., and Erali, D. R., 1974, "Larger Diameter Underwater Pipeline for Nuclear Power Plant Designed Against Soil Liquefaction," *OTC*, Vol. 2, pp. 597-602.
- Lee, K. L., and Chan, K., 1972, "Number of Equivalent Significant Cyclones in Strong Motion Earthquakes," *Proceedings of the International Conference on Microzonation*, University of Washington, Seattle, pp. 609-627.
- McDougal, W. G., Liu, P. L., Tsai, Y. T., and Clukey, E., 1989, "Wave-Induced Pore Pressure Accumulation in Marine Soil," *ASME JOURNAL OF OFFSHORE MECHANICS AND ARCTIC ENGINEERING*, Vol. 111, pp. 1-11.
- McDougal, W. G., and Liu, P. L., 1986, "Wave-Induced Pore Pressure Accumulation in Marine Soils," *Proceedings 5th International OMAE*, Vol. 1, pp. 574-581.
- Rahman, M. S., and Layas, F. M., 1986, "Pore Pressure in Ocean-Floor Sands Under Random Waves," *Marine Geotechnology*, Vol. 6, pp. 341-358.
- Seed, H. B., and Idriss, I. M., 1967, "Analysis of Soil Liquefaction: Nigata Earthquake," *Journal of Soil Mechanics and Foundations Division*, ASCE, Vol. 93, pp. 83-108.
- Seed, H. B., and Rahman, M. S., 1978, "Wave-Induced Pore Pressure in Relation to Ocean Floor Stability of Cohesionless Soils," *Marine Geotechnology*, Vol. 3, pp. 123-150.